Supplementary Materials for

Vasopressin/Oxytocin-Related Signaling Regulates Gustatory Associative Learning in *Caenorhabditis elegans*

Isabel Beets, Tom Janssen, Ellen Meelkop, Liesbet Temmerman, Nick Suetens, Suzanne Rademakers, Gert Jansen, Liliane Schoofs*

.

*To whom correspondence should be addressed. E-mail: liliane.schoofs@bio.kuleuven.be

This PDF file includes:

Other Supplementary Materials for this manuscript includes the following:

Materials and Methods

Nematode strains and culture conditions

C. elegans were cultured at 20 or 25°C under standard conditions and fed *E. coli* OP50 (*22*). Wild type worms were Bristol variety N2.

The following mutant strains were used (x times outcrossed to N2): LSC42 *ntc-1 (tm2385)* X (3x), LSC48 *ntr-1(tm2765)* I (4x), LSC46 *ntr-1(ok2780)* I (2x), LSC47 *ntr-2 (tm2243)* X (1x), CX10 *osm-9(ky10)* IV, NL792 *gpc-1(pk298)* X (6x), CB1112 *cat-2 (e1112)* II, MT15434 *tph-1(mg280)* II (kindly provided by M. Alkema, University of Massachusetts Medical School, Worcester, MA), GJ2258 *ntr-1(tm2765)* I*; gpc-1(pk298)* X, GJ2260 *ntc-1(tm2385)* X*; gpc-1(pk298)* X, GJ2263 *ntr-1(tm2765)* I*; cat-2(e1112)* II, GJ2262 *ntc-1(tm2385)* X*; cat-2(e1112)* II, GJ2261 *ntr-1(tm2765)* I*; tph-1(mg280)* II, GJ2259 *ntc-1(tm2385) X; tph-1(mg280)* II, LSC275 *ntr-1(tm2765)* I; *ntr-2(tm2243)* X.

The following transgenic strains were used in this work: LSC309-310, *lstEx233-234 [*P*ntc-1::ntc-1::gfp]*; LSC311-312, *lstEx235-236 [*P*ntr-1::ntr-1::gfp]*; LSC313, *lstEx237 [*P*ntr-2::ntr-2::gfp]*; LSC314-316, *lstEx238-240 [*P*ntc-1::ntc-1 SL2 gfp]*; LSC317-318, *lstEx241-242 [*P*ntr-1::ntr-1 SL2 gfp]*; LSC115-116, *lstEx38-39 [*P*ntc-1::gfp]*; LSC110, LSC113, *lstEx33, lstEx36 [*P*ntr-1::gfp]*; LSC75, LSC76, *lstEx70, lstEx186 [*P*ntr-2::gfp]*; LSC277-282, *ntc-1(tm2385)* X, *lstEx201-206 [*P*odr-2::ntc-1 SL2 gfp]*; LSC283-286, *ntc-1(tm2385)* X, *lstEx207-210 [*P*lin-11::ntc-1 SL2 gfp]*, LSC287-289, *ntc-1(tm2385)* X, *lstEx211-213 [*P*unc-86::ntc-1 SL2 gfp]*; LSC290-292, *ntc-1(tm2385)* X, *lstEx214-216 [*P*gpa-2::ntc-1 SL2 gfp]*; LSC293-294, *ntc-1(tm2385)* X, *lstEx217-218 [*P*gcy-8::ntc-1 SL2 gfp]*; LSC295-298, *ntc-1(tm2385)* X, *lstEx219-222 [*P*nlp-12::ntc-1 SL2 gfp]*; LSC299-302, *ntc-1(tm2385)* X, *lstEx223-226 [*P*flp-1::ntc-1 SL2 gfp]*; CX14273-14274, F39C12.4(*tm2385*) X, *kyEx4522-4523 [*P*tph-1::*F39C12.4 *SL2 gfp]* (kindly provided by C. Bargmann, Rockefeller University, New York, NY); LSC179-180, LSC228, LSC241, *ntr-1(tm2765)* X, *lstEx102-103, lstEx154, lstEx167 [*P*gcy-7::ntr-1]*; LSC151-155 *ntr-1(tm2765)* X, *lstEx74-78 [*P*sra-6::ntr-1]*; LSC303-308, *ntr-1(tm2765)* X, *lstEx227-232 [*P*srh-142::ntr-1 SL2 gfp]*; LX960 *lin-15B(n765)* X, *vsIs97 [*P*tph-1::DsRed2, lin-15(+)]*; NY2067 *him-5(e1490)* V, *ynIs67 [*P*flp-6::gfp]* III.

Molecular biology

Plasmids used for receptor expression in mammalian cells were constructed by cloning the *ntr-1* and *ntr-2* cDNAs into the eukaryotic expression vector pcDNA3.1D (Invitrogen) as previously described (*23*). Primers used for the PCR amplification of each cDNA were: F: 5'-caccatgggagccttctttcctg-3' and R: 5'-tcaaaaatcgctttgctcactgg-3' for *ntr-1* cDNA, F: 5'-caccatgaacaacaacacg-3' and R: 5'-tcgagttaattagagttggtcttc-3' for *ntr-2*

cDNA. Each receptor cDNA sequence was confirmed to be identical to the predicted sequence (www.wormbase.org).

The construct for GFP-tagged NTR-2, used to verify membrane targeted receptor expression in mammalian cells, was generated by adding *Hind*III and *Kpn*I sites to the *ntr-2* cDNA by means of PCR and cloning the resulting amplicon in frame with a GFP coding sequence in the pEGFP-N1 vector (Clontech).

The translational *ntc-1* reporter transgene was constructed by cloning a genomic DNA fragment, including the full-length *ntc-1* ORF and 3.6 kb of sequence upstream from the start codon, into the GFP expression vector pPD95.75 between the *Hind*III and *BamH*I sites. A similar construct was generated for *ntr-1* by cloning the full-length *ntr-1* ORF and 4 kb of the upstream promoter sequence between the *Pst*I and *Age*I sites. Due to the large size of the genomic *ntr-2* coding sequence, a translational *ntr-2* reporter transgene was constructed by fosmid recombineering (*24*). pBALU1 was used as template for the amplification of the GFP reporter cassette, which was then inserted at the C-terminus of the *ntr-2* ORF in fosmid WRM062aE11. Because of the low expression levels of full-length GFP-tagged NTC-1 and NTR-1, additional reporter constructs were generated in a modified pSM vector carrying a GFP reporter sequence preceded by an SL2 trans-splicing sequence (kindly provided by C. Bargmann, Rockefeller University, New York, NY). *ntc-1* genomic DNA or *ntr-1* cDNA was cloned between the *Sal*I and *Kpn*I sites of the pSM vector, while corresponding promoters were cloned between the *Fse*I and *Asc*I sites. The expression patterns were confirmed to be identical to the patterns of full-length GFP-tagged NTC-1 and NTR-1. Transcriptional *ntr-1*, *ntr-2* and *ntc-1* reporter transgenes were created by overlap extension PCR (*25*) using genomic DNA as template for the amplification of 4, 3.5 and 3.6 kb of promoter sequence, respectively. For *ntc-1*, an additional DNA sequence encoding the first 95 of 104 amino acids of the predicted NTC-1 was incorporated. Expression patterns of transcriptional reporter transcripts were confirmed to be identical to those of full-length GFP-tagged proteins, but *ntc-1* expression from a transcriptional construct was also found in a number of additional unidentified cells.

To generate cell-specific rescue constructs, *ntc-1* genomic DNA or *ntr-1* cDNA was first cloned between the *Sal*I and *Kpn*I sites of the pSM SL2 GFP vector. The following promoters were then cloned between the *Fse*I and *Asc*I sites: *odr-2 (2b)*, *lin-11 (DE)*, *unc-86*, *gpa-2*, *gcy-8*, *nlp-12*, *flp-1* and *srh-142 (23, 26-32)*, and expression patterns of GFP reporters were verified. For the P*flp-1::ntc-1 SL2 gfp* transgene, strong GFP reporter expression was found in AVK neurons and minor background expression in few additional non-*ntc-1* expressing cells. ASH- and ASEL-specific *ntr-1* rescue constructs were generated using overlap extension PCR by fusing a genomic region corresponding to the entire coding sequence of *ntr-1* to the *sra-6* or *gcy-7* promoter (both amplified by PCR from genomic DNA), respectively (*30, 33*).

Genomic DNA used as template in PCR was isolated from wild type mixed stage worms.

Peptides

A peptide library of 262 synthetic *C. elegans* peptides was composed based on *in silico* predictions and in-house peptidomics data (*34*), and custom synthesized by Thermo Scientific and Eurogentec. VP/OT-related peptides from non-nematode species were synthesized by GL Biochem Ltd. (GLS). HPLC fractionated peptide extracts, used in additional NTR-2 ligand screening experiments, were prepared from whole mount mixed stage *C. elegans* according to (*35*). Pattern-based database searches of proteins encoded by the *C. elegans* genome did not reveal any additional VP/OT-related precursor candidates besides NTC-1.

Receptor deorphanization assay

Chinese hamster ovary (CHO) cells K1 stably overexpressing the mitochondrial targeted apo-aequorin (mtAEQ) and the human $G\alpha_{16}$ subunit were cultured and transfected with pcDNA3.1D-*ntr-1* or pcDNA3.1D-*ntr-2* as described in (*23*). Cells for negative control experiments were transfected with an empty pcDNA3.1D vector. Cells used in coexpression studies were transfected with a 1:1 ratio of pcDNA3.1D-*ntr-1* and pcDNA3.1D-*ntr-2*, or as a control with pcDNA3.1D-*ntr-1* and the empty pcDNA3.1D vector. All peptides from the library were initially tested at a concentration of 10^{-5} M. Receptor activating peptides were HPLC purified (*23*) and tested in final concentrations from 10^{-4} to 10^{-12} M. Calcium responses were monitored as previously described (*23*) for 30 seconds on a Mithras LB 940 luminometer (Berthold Technologies). Dose-response measurements were always conducted in triplicate and for at least two independent experiments. Half maximal effective concentrations (EC_{50} values) were calculated from dose-response curves that were constructed using a computerized nonlinear regression analysis with a sigmoidal dose-response equation (SigmaPlot 12.0). Receptor responses to all peptides were verified with a second independent calcium mobilization assay using human embryonic kidney (HEK) 293T cells (*36*). For NTR-2, additional assays were performed with HPLC fractions of a whole body peptide extract of mixed stage worms.

Pharmacological receptor characterization

Calcium responses in receptor expressing CHO-K1 cells, stably overexpressing mtAEQ but lacking the human $G\alpha_{16}$ subunit, were measured on a Mithras LB 940 luminometer as described above.

cAMP responses were monitored in receptor expressing HEK293T cells that were cotransfected with a multimerized *cyclic AMP response element (CRE) luciferase* reporter construct in a 1:1 (*luciferase* reporter:receptor) ratio. Two days post-transfection,

cells were challenged for 4 hours at 37°C with peptides dissolved in serum-free medium supplemented with 200 µ M of 3-isobutyl-1-methylxanthine (IBMX). Forskolin was added at 10 µM to test for $G\alpha_i$ activity. Quantification of the luciferase activity was done using the SteadyLitePlus kit (PerkinElmer Life Sciences) according to the manufacturer's instructions, and luminescence was measured on a Mithras LB 940 luminometer.

Transgenesis and expression pattern analysis

Germline transformations were carried out by standard microinjection techniques as described (*37*). GFP reporter constructs for expression analysis were injected into wild type animals at 50 ng/µl with P*elt-2::mCherry* as coinjection marker. Rescue constructs were injected into the *ntr-1(tm2765)* or *ntc-1(tm2385)* background at multiple concentrations ranging from 5 up to 50 ng/µl using the P*elt-2::gfp* transgene as selection marker and L4440 vector as carrier DNA. Final concentrations of total injected DNA were 100 ng/µl. At least two independent lines from each injection were generated and analyzed for expression patterns and behavioral assays.

The expression patterns of GFP reporter transgenes were visualized by an Olympus Fluoview FV1000 (IX81) confocal microscope. Confocal Z-stack projections were exported through Imaris 7.2 (Olympus). Cells were identified by Nomarski DIC microscopy (on a Zeiss Axio Imager.Z1 microscope) at L1 stage based on their position, morphology and DiI/FITC staining (*38*). Expression in NSM neurons was confirmed by colocalization with P*tph-1::DsRed2* and in ASE and AFD neurons by colocalization with P*flp-6::gfp*. Except for variation in expression levels or unless indicated otherwise, all GFP reporter lines showed similar expression patterns.

Behavioral assays

Chemotaxis towards NaCl and gustatory plasticity were assessed as previously described (*16, 39*). In brief, assays were performed on four-quadrant Petri plates (Falcon X plate, Becton Dickinson Labware). Pairs of opposite quadrants were filled with buffered agar (2% agar, 5 mM KH_2PO_4/K_2HPO_4 pH 6.6, 1 mM $CaCl_2$ and 1 mM $MgSO_4$) supplemented with NaCl in one of both quadrant pairs. Assay plates were always prepared fresh and left open on the bench top to solidify and dry for 60 minutes. Plates were then closed and stored for use on the same day. Animals for behavioral assays were maintained on fresh (less than one week old) culture plates seeded with sufficient *E. coli* OP50. Because chemotaxis and gustatory plasticity assays are sensitive to ambient conditions including air humidity, care was taken to standardize experimental procedures and the behavior of animals was always compared with that of positive (*osm-9(ky10)* animals (*18*)) and negative (wild type) controls performed on the same day(s). Salt chemotaxis was tested using 0.1, 1, 10, 100, 200, 300 or 500 mM or 1 M NaCl. Well fed, young adult nematodes were washed off plates with CTX buffer (5 mM

KH_2PO_4/K_2HPO_4 pH 6.6, 1 mM $CaCl_2$ and 1 mM $MgSO_4$) and washed three times in the same buffer solution over a period of 15 minutes. 100-200 worms were placed at the intersection of the four-quadrant assay plate and the distribution of animals over the quadrants was determined at 10 minutes. The chemotaxis index was calculated: (A-C)/(A+C), where A is the number of worms within the quadrants containing 25 mM NaCl and C is the number of worms within the control quadrants (no NaCl). Animals for gustatory plasticity assays were washed three times during 15 minutes in CTX buffer containing 0 mM (naive animals) or 100 mM NaCl (NaCl-conditioned animals). 100-200 pre-exposed animals were placed at the intersection of the four-quadrant assay plate and tested for chemotaxis. The distribution of worms over the four quadrants was determined at 10 minutes and the chemotaxis index was calculated as described above.

Starvation-enhanced gustatory plasticity was tested by starving animals on CTX plates for 1 to 4 hours prior to the gustatory plasticity assay (*17*).

Supplementation studies with dopamine and serotonin were carried out as described previously (*17*). Briefly, animals were cultured for 4 (short-term) or 72 (including larval development) hours before the assay on seeded NGM-plates containing either 2 mM dopamine hydrochloride or serotonin creatinine sulfate complex. For each substance, the applied concentration of 2 mM did not influence the behavior of wild type animals.

Statistical significance of salt chemotaxis and gustatory plasticity assays was determined using one-way ANOVA and Tukey post-hoc for multiple comparisons. For supplementation studies with dopamine and serotonin, statistical significance was determined based on the coefficients of a linear model, fitting chemotaxis index as a function of strain, condition (hours on dopamine or serotonin) and their interaction, and correcting for variation between different days. All chemotaxis assays were conducted at least four times and on at least two separate days.

Phylogenetic analysis

A protein data set of 28 unique amino acid sequences of VP/OT- and GnRH-related receptors, originating from several vertebrate and invertebrate species, was composed (Table S1). To select the optimal protein model of molecular evolution, ProtTest v. 2.4 (*40-42*) was used through the online platform Phylemon v.2.0 (*43*). In view of its availability in MrBayes v.3 (*44, 45*), the second best model according to the Akaike Information Criterion (AIC) (*46*), namely the WAG model (*47*), with a gamma shape parameter of 1.3 and a proportion of invariable sites of 0.015, was used for Bayesian inference (BI) of phylogeny. Posterior probabilities were calculated over 4 million generations, sampling every 100 generations and discarding 25% of samples as “burn-in”.

Statistical tests

The R 2.14.0 software package was used for statistical tests on all data (*48*).

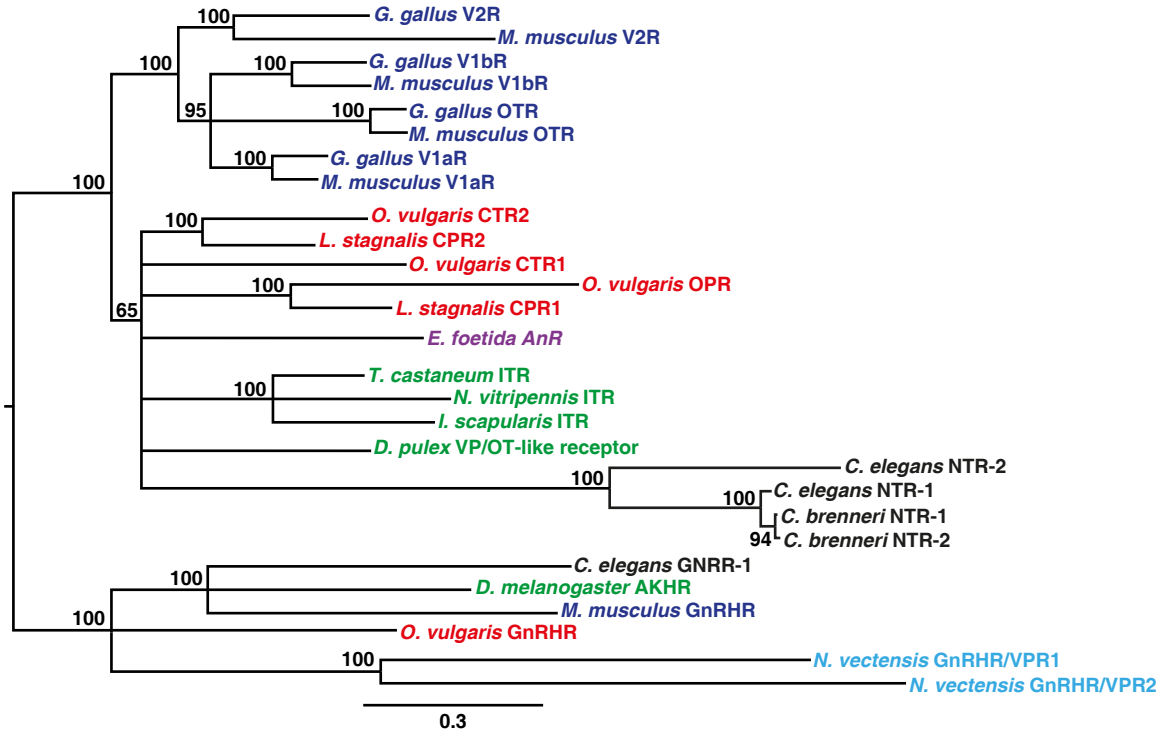

Fig. S1.

Bayesian inferred phylogenetic relationships of *C. elegans* nematocin receptors NTR-1 and NTR-2 with members of the VP/OT receptor family and closely related gonadotropin releasing hormone receptor (GnRHR) family. Nematocin receptors cluster in the VP/OT receptor clade, while receptors of the GnRHR family including *C. elegans* GNRR-1 are outgrouped with strong support. Receptors from vertebrates, dark blue; mollusks, red; arthropods, green; annelids, purple; nematodes, black; cnidarians, light blue. Posterior probabilities are given as percentages at each node. Branch lengths indicate the expected number of substitutions per site. Abbreviations and accession numbers of sequences are summarized in Table S1.

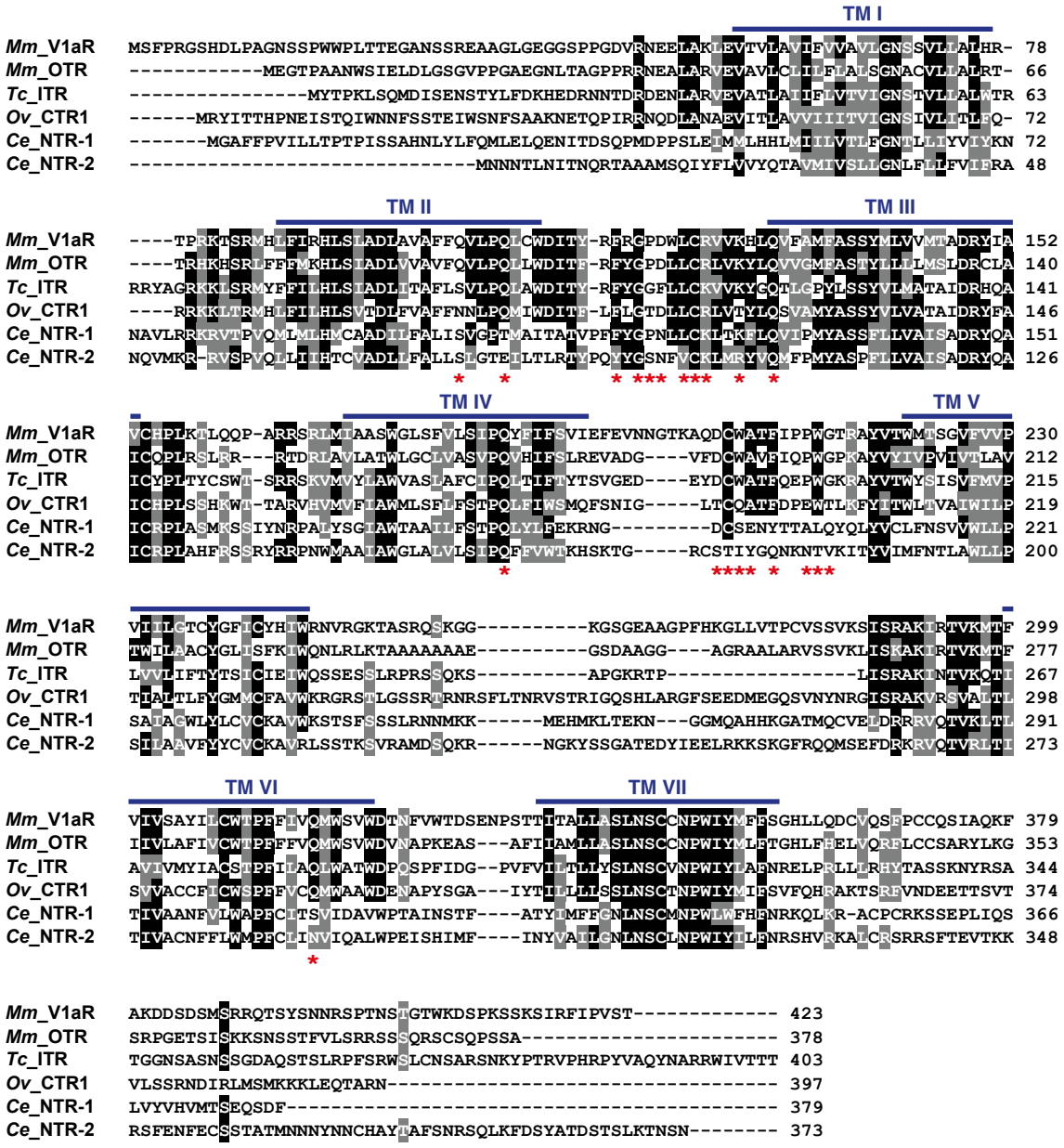

Fig. S2.

Conservation of VP/OT receptor features in NTR-1 and NTR-2. Amino acid sequence alignment of *C. elegans* nematocin receptors NTR-1 (*Ce*_NTR-1) and NTR-2 (*Ce*_NTR-2), mouse vasopressin V1a receptor (*Mm*_V1aR) and oxytocin receptor (*Mm*_OTR), *Tribolium castaneum* inotocin receptor (*Tc*_ITR) and *Octopus vulgaris* cephalotocin receptor 1 (*Ov*_CTR1). Asterisks mark conserved residues suggested to be important for receptor-ligand interactions in vertebrate VP/OT receptors (*49, 50*). Identical residues, black; similar residues, grey; putative transmembrane (TM) domains, blue bars. Accession numbers of sequences are summarized in Table S1.

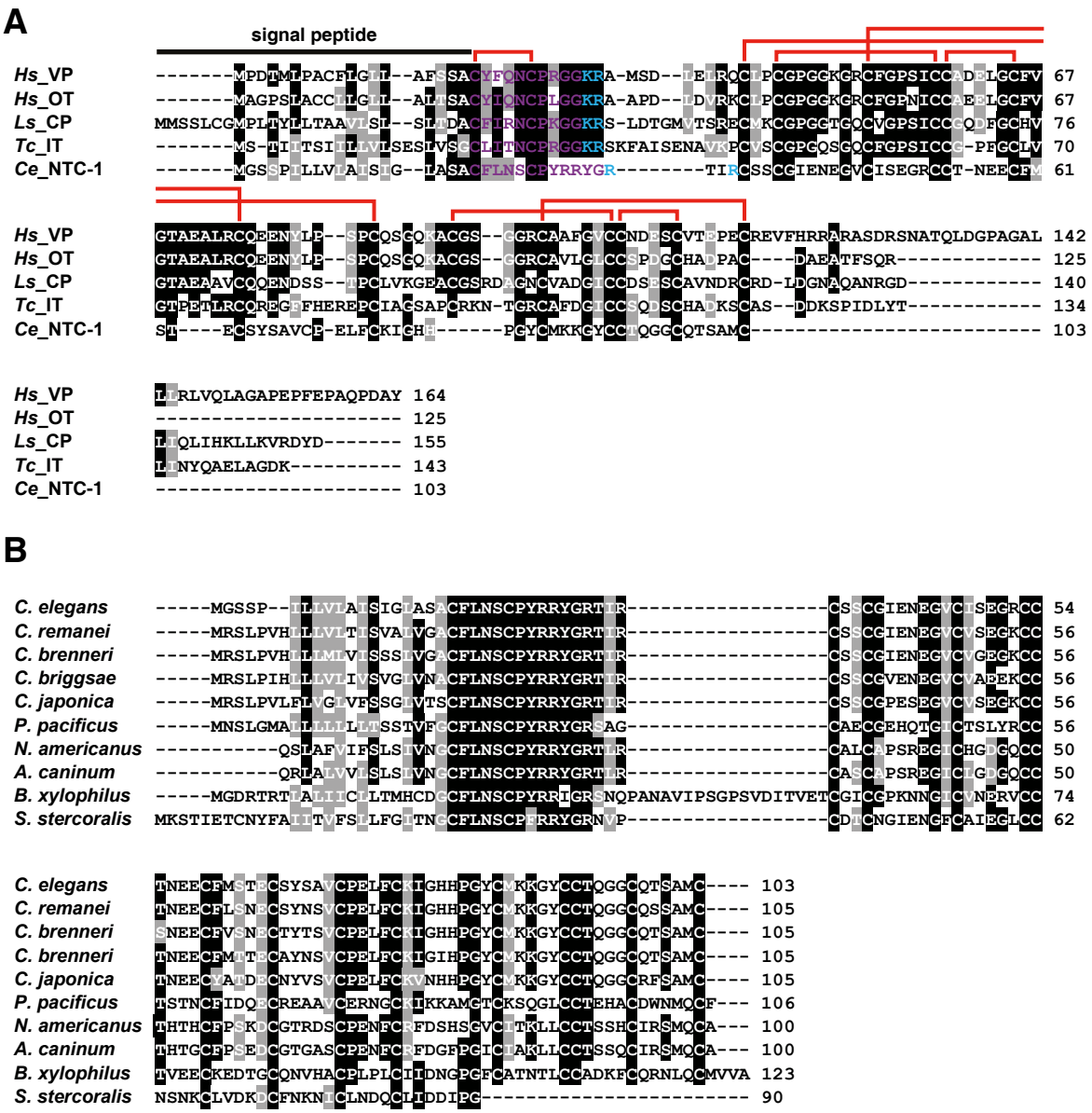

Fig. S3.

Conservation of VP/OT precursor features in nematocin precursors. (**A**) Amino acid sequence alignment of precursors for *C. elegans* nematocin (*Ce*_NTC-1), human vasopressin (*Hs*_VP) and oxytocin (*Hs*_OT), *Lymnea stagnalis* conopressin (*Ls*_CP) and *Tribolium castaneum* inotocin (*Tc*_IT). Identical residues, black; similar residues, grey; VP/OT-like peptides, purple; proprotein convertase sites, blue; disulfide bridges, red. (**B**) Amino acid sequence alignment of NTC-1 precursor homologs in nematode species. Nematocin precursor sequences from *N. americanus*, *A. caninum*, *S. stercoralis* and *B. xylophilus* were derived from EST sequences and may be incomplete. Box shading as in (A). Full species names and accession numbers are summarized in Table S3.

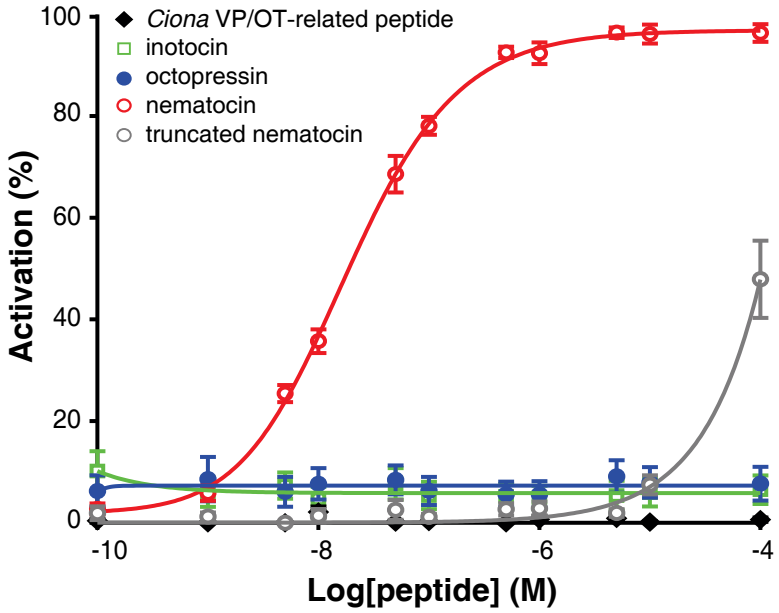

Fig. S4.

NTR-1 is only activated by the full-length nematocin peptide. Dose-response curves of calcium responses evoked in NTR-1 expressing CHO cells by the VP/OT-like peptides inotocin (CLITNCPRGamide), octopressin (CFWTSCPIGamide), *Ciona* VP/OP-related peptide (CFFRDCSNMDWYR), nematocin (CFLNSCPYRRYamide) and C-terminally truncated nematocin (CFLNSCPY). Dose-response data are represented as relative (%) to the highest value (100% activation) after normalization to the maximum calcium response. Error bars represent SEM ($n \geq 3$).

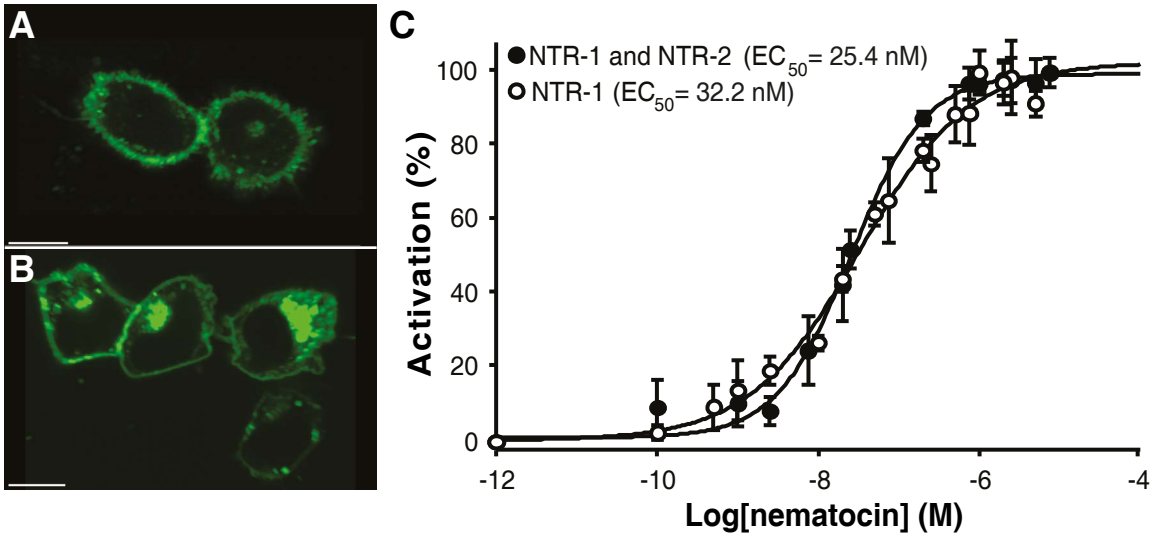

Fig. S5.

NTR-2 expression verification and cotransfection studies in mammalian cells. (**A**) Confocal image of GFP-tagged NTR-2 expression at the plasma membrane of CHO and (**B**) HEK293T cells. (**C**) Dose-response curves of calcium responses evoked by nematocin in NTR-1 expressing CHO cells with or without coexpression of NTR-2. Dose-response data are represented as relative (%) to the highest value (100% activation) after normalization to the maximum calcium response. Scale bars represent 10 μm. Error bars represent SEM ($n \geq 3$).

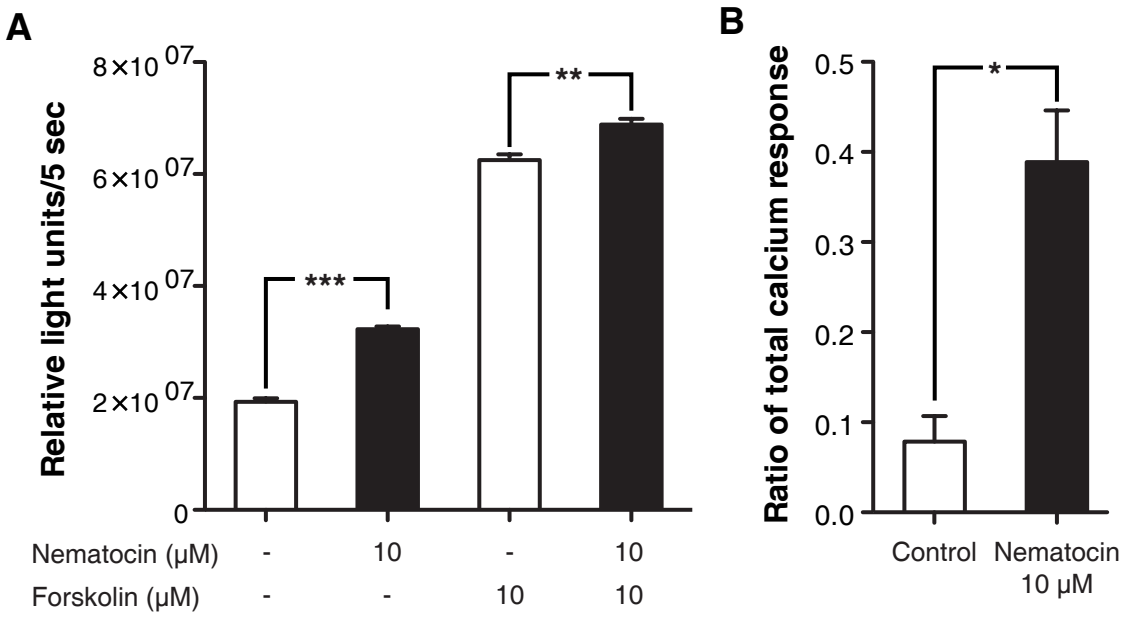

Fig. S6.

Activation of NTR-1 affects intracellular cAMP and calcium levels. (**A**) cAMP levels measured in NTR-1 expressing HEK293T cells as relative light units/5 sec emitted by a CRE luciferase reporter in the absence or presence of nematocin. Forskolin was added to stimulate cAMP production and test for a decrease in cAMP levels resulting from $G\alpha_i$ activity. (**B**) Calcium levels measured in NTR-1 expressing CHO cells lacking $G\alpha_{16}$ in the absence (control) or presence of nematocin. Values are reported as the ratio of the total calcium response. Statistical significance was determined using one-way ANOVA and Tukey post-hoc comparison. $*P < 0.05$, $**P < 0.01$, $***P < 0.001$. Error bars indicate SEM ($n \geq 3$).

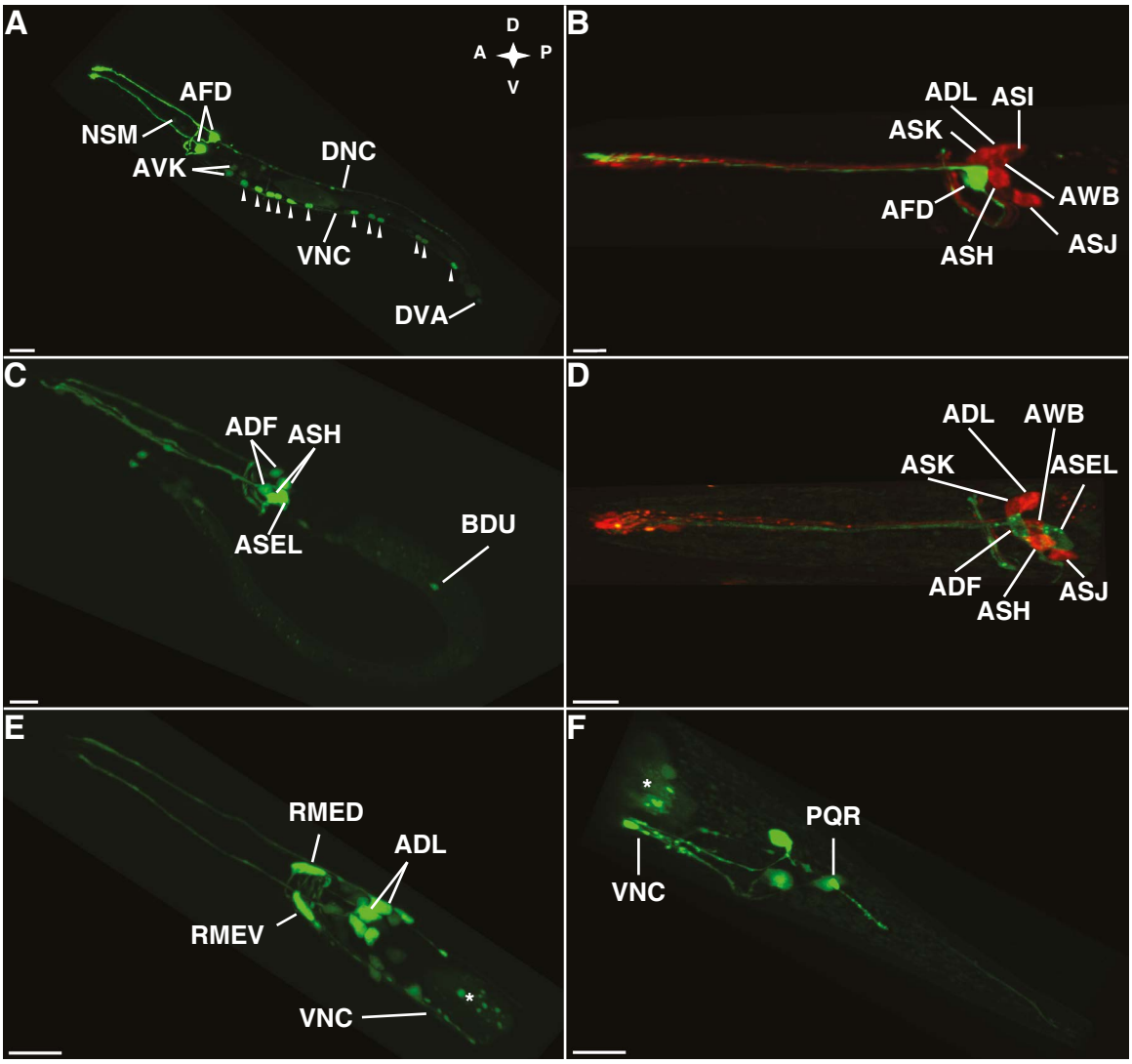

Fig. S7.

Labeled confocal Z-stack projections showing overall expression patterns of *ntc-1*, *ntr-1* and *ntr-2* in L1 hermaphrodites. (**A**) and (**B**) Expression of the *ntc-1::gfp* transgene was additionally observed in NSM neurosecretory motor neurons and motor neurons along the ventral nerve cord (indicated by arrow heads). Occasionally expression was found in two paired head neurons that might be identified as ASG and AIZ (unassigned). (**C**) and (**D**) Expression of the *ntr-1::gfp* transgene was additionally observed in the body cavity neuron BDU and most likely the tail neuron PQR (unassigned). (**E**) and (**F**) Expression of the *ntr-2::gfp* transgene in the head and tail region, respectively. *ntr-2* expression was identified in the ADL sensory neurons, the RMED and RMEV motor neurons and most likely the PQR tail neuron. (**B**) and (**D**) Head regions showing *ntc-1::gfp* and *ntr-1::gfp* transgene expression (green), respectively, and DiI stained amphid neurons (red). Asterisks mark fluorescence in the intestine from the coinjection marker P*elt-2::mCherry*. Scale bars represent 10 µm. VNC, ventral nerve cord; DNC, dorsal nerve cord.

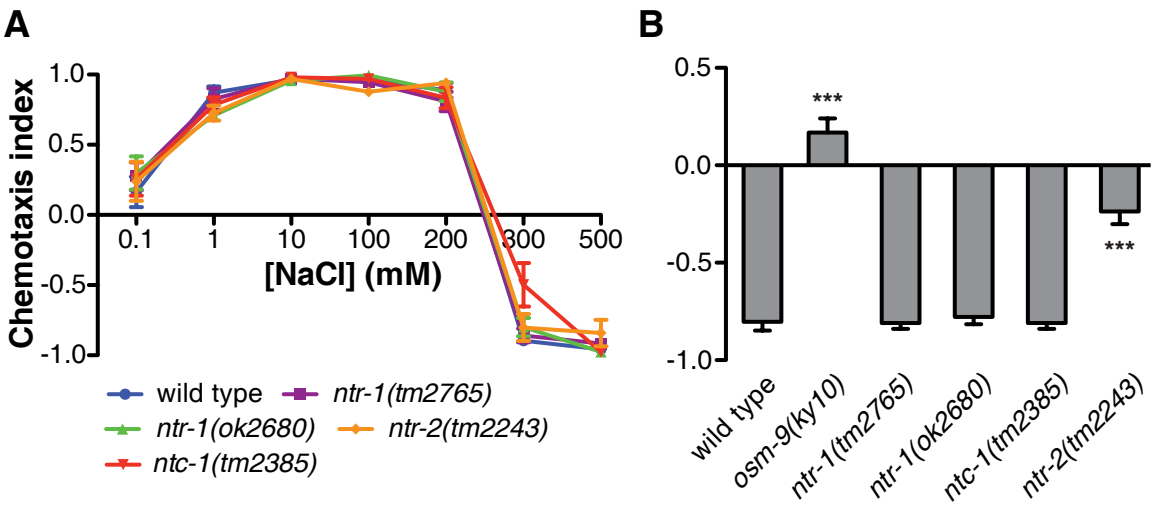

Fig. S8.

Mutants defective in nematocin signaling display normal salt chemotaxis and osmotic avoidance. (**A**) Mean chemotaxis behaviors of naive wild type animals and *ntr-1*, *ntr-2* and *ntc-1* mutants to increasing NaCl concentrations. (**B**) Osmotic avoidance behavior of wild type and *ntr-1*, *ntr-2* and *ntc-1* mutant animals. The mean chemotaxis index towards 1M NaCl of naive animals is plotted. *osm-9(ky10)* animals, which are impaired in osmotic avoidance behavior (*51*), were used as positive control. Statistical significance was determined using one-way ANOVA and Tukey post-hoc comparison. Error bars represent SEM ($n \geq 4$). ***$P < 0.001$.

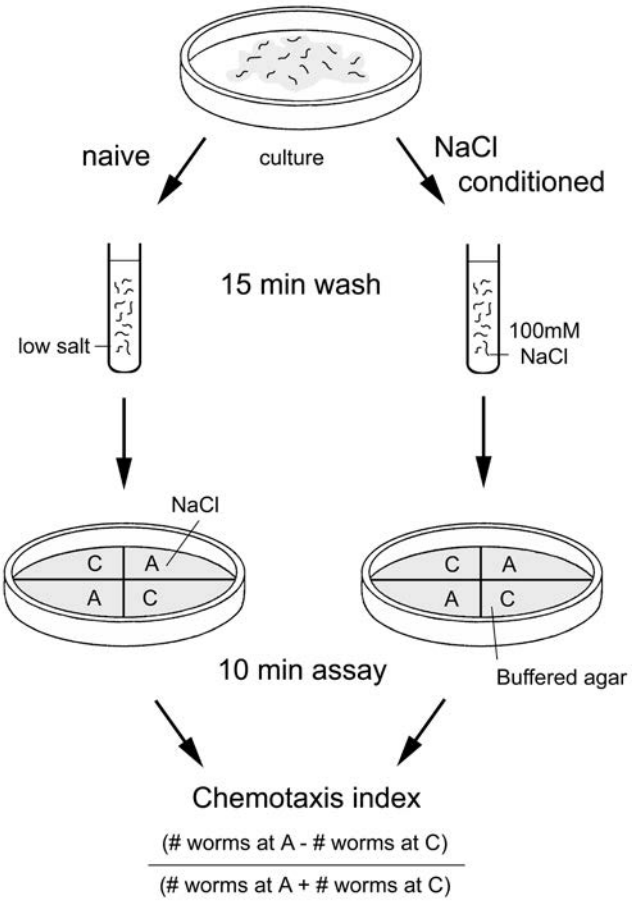

Fig. S9.

Gustatory plasticity assay. Worms are washed off plates in low-salt buffer (0 mM NaCl, naive animals) or buffer containing an attractive NaCl concentration (100 mM NaCl, NaCl-conditioned animals) for 15 minutes and tested for chemotaxis. The assay plates contain two control quadrants filled with buffered agar (C) and two test quadrants (A) supplemented with 25 mM NaCl. The distribution of animals over the four quadrants is determined after 10 minutes, and the corresponding chemotaxis index is calculated.

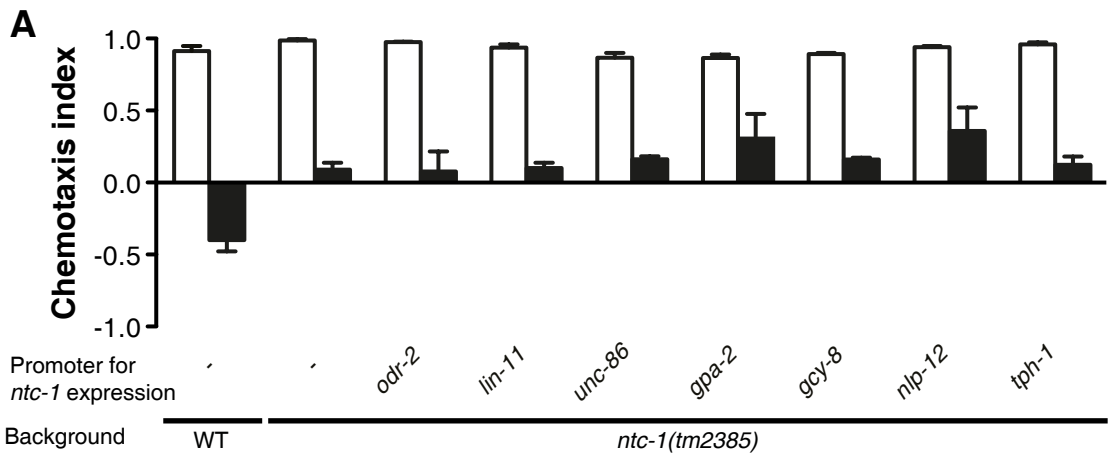

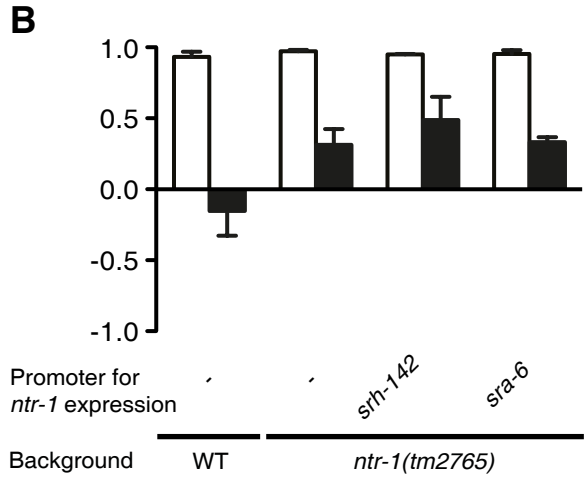

C

P::*ntc-1*	Expression pattern
ntc-1	AFD, DVA, NSM, M5, AVK, AIZ?, ASG?
odr-2	AIB, AIZ, ASG, AVG, IL2, PVP, RIV, SIAV
lin-11	ADF, ADL, AIZ, AVG, AVH/AVJ, RIC, PHA, PVQ
unc-86	ADA, AIM, AIZ, ALM, ALN, BDU, FLP, HSN, IL2, NSM, PLM, URY
gpa-2	AIA, AWC, PHA, PHB, PVT, M1, M5, I5
gcy-8	AFD
nlp-12	DVA
tph-1	NSM, ADF, HSN

P::*ntr-1*	Expression pattern
ntr-1	ADF, ASH, ASEL, PQR
srh-142	ADF
sra-6	ASH, ASI

Fig. S10.

ntc-1 and *ntr-1* rescue experiments. (**A**) The *ntc-1* gene was expressed in the *ntc-1(tm2385)* background driven by promoters specific to selected cells, and gustatory plasticity of transgenic animals was assessed. (**B**) *ntr-1* cDNA was expressed in the *ntr-1(tm2765)* background driven by the *sra-6* or *srh-142* promoter, and transgenic animals were subjected to the gustatory plasticity assay. (**C**) Summary of neural expression patterns of promoters used for *ntc-1* and *ntr-1* rescue experiments in (A) and (B). Cells overlapping with *ntc-1::gfp* and *ntr-1::gfp* transgene expression are marked in red. No significant difference from *ntc-1(tm2385)* and *ntr-1(tm2765)* mutant behaviors was found using one-way ANOVA and Tukey post-hoc comparison. For all behavioral rescue assays, at least two independent lines were tested and representative data from one line is plotted. Error bars represent SEM ($n \geq 4$).

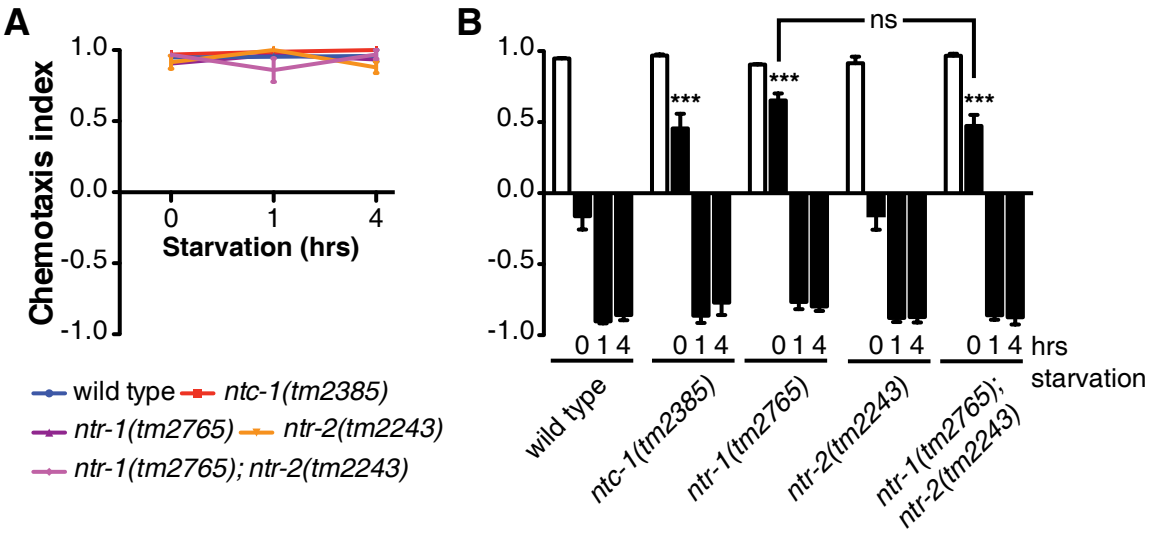

Fig. S11.

Starvation prior to the learning assay induces a nematocin-independent mechanism for gustatory plasticity. (**A**) Responses of naive wild type animals and *ntr-1(tm2765)*, *ntc-1(tm2385)*, *ntr-2(tm2243)* and *ntr-1(tm2765); ntr-2(tm2243)* mutants to 25 mM NaCl that were starved for 0-4 hours on CTX plates prior to the assay. (**B**) Wild type and mutant animals were starved for 0-4 hours on CTX plates, and subjected to the gustatory plasticity assay. The mean chemotaxis index towards 25 mM NaCl of naive (0 hours starved, open bars) and NaCl-conditioned (0-4 hours starved, filled bars) animals is plotted. Statistical significance compared to wild type was determined using one-way ANOVA and Tukey post-hoc comparison. ***$P < 0.001$. Error bars represent SEM ($n \geq 4$); ns, not significant.

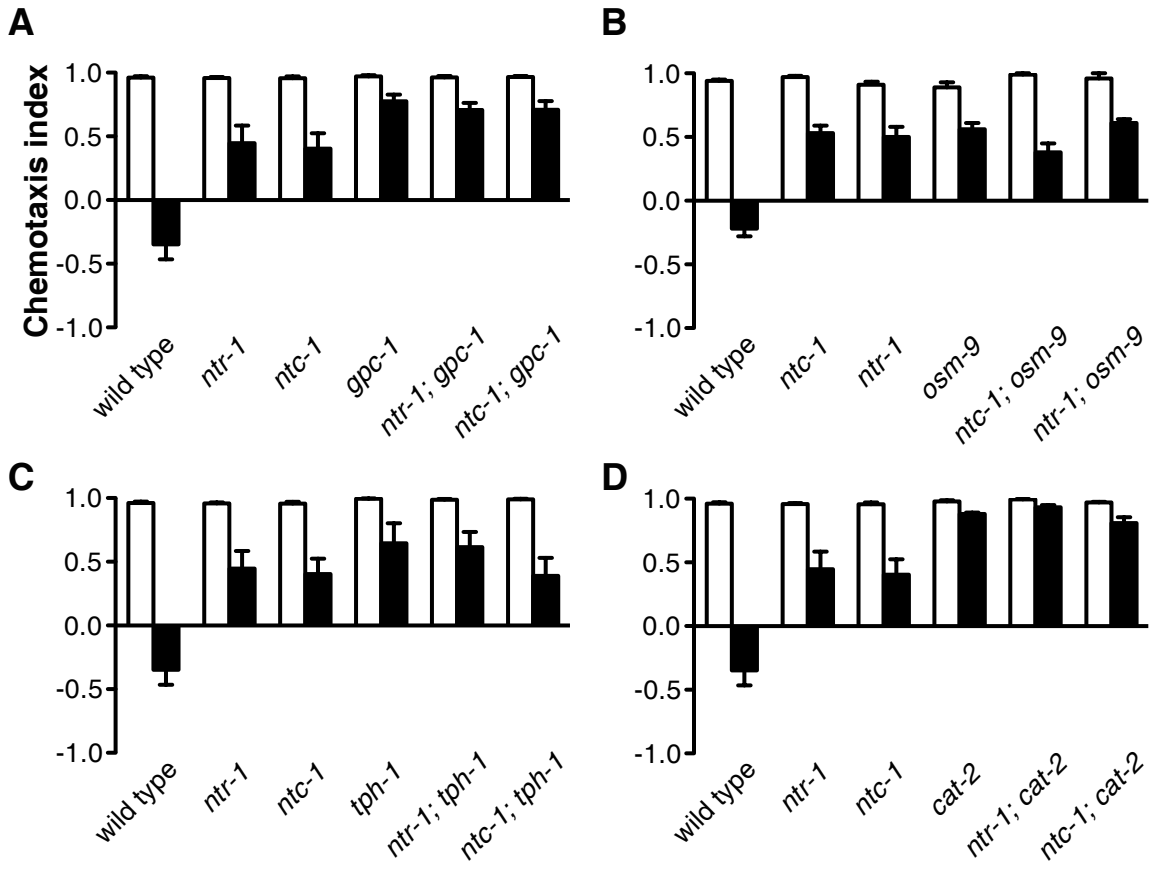

Fig. S12.

Nematocin signaling acts in the same genetic pathway as *gpc-1*, *osm-9*, *tph-1* and probably *cat-2*. (**A-D**) The mean chemotaxis index towards 25 mM NaCl of naive (open bars) and NaCl-conditioned (filled bars) animals is plotted for wild type, *ntr-1(tm2765)*, *ntc-1(tm2385)*, *gpc-1(pk298)*, *osm-9(ky10)*, *tph-1(mg280)*, *cat-2(e1112)* and their corresponding double mutants. Statistical significance was determined using one-way ANOVA and Tukey post-hoc comparison. For (**D**), NaCl-conditioned behaviors of *ntr-1; cat-2* and *ntc-1; cat-2* animals differed from *ntr-1* and *ntc-1* single mutants with marginal significance ($P < 0.05$), and were inconclusive because of the severe plasticity defect of *cat-2* single mutants. Error bars represent SEM ($n \geq 4$).

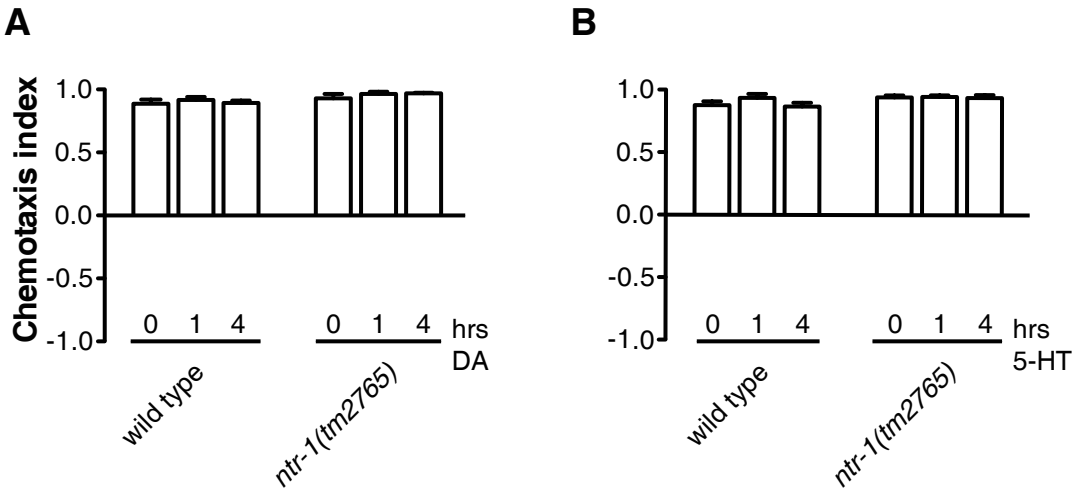

Fig. S13.

Dopamine or serotonin exposure does not affect responses of naive animals. The mean chemotaxis index towards 25 mM NaCl of naive wild type and *ntr-1(tm2765)* mutant animals 0-4 hours after exposure to 2 mM of (**A**) dopamine or (**B**) serotonin is plotted. Error bars represent SEM ($n \geq 4$). DA, dopamine; 5-HT, serotonin.

Table S1.

Abbreviations and accession numbers of receptor sequences in the phylogenetic dataset.

Abbreviation	Full name	Species	Accession number
AKHR	Adipokinetic hormone receptor	*Drosophila melanogaster*	AAC61523.1
AnR	Annetocin receptor	*Eisenia foetida*	Q75W84.1
CPR	Conopressin receptor	*Lymnea stagnalis*	AAA91998.1, AAC46987.1
CTR	Cephalotocin receptor	*Octopus vulgaris*	Q7YW31.1, Q5WA50.1
GnRHR	GnRH receptor	*Mus musculus*, *Octopus vulgaris*	NP_034453.1, Q2V2K5.1
GnRHR/VPR	GnRH/VP-like receptor	*Nematostella vectensis*	201906, 209131[a]
GNRR	GnRH-related receptor	*Caenorhabditis elegans*	CCD68969.1
ITR	Inotocin receptor	*Tribolium castaneum*, *Nasonia vitripennis*, *Ixodes scapularis*	NP_001078830.1, NP_001165745.1, XP_002399500.1
NTR	Nematocin receptor	*Caenorhabditis elegans*, *Caenorhabditis brenneri*	AFJ42569, AFJ42490, EGT31406.1, EGT47432.1
OPR	Octopressin receptor	*Octopus vulgaris*	Q5W9T5.1
OTR	Oxytocin receptor	*Mus musculus*, *Gallus gallus*	NP_001074616.1, NP_001026740.1
V1aR	Vasopressin 1a receptor	*Mus musculus*, *Gallus gallus*	NP_058543.2, NP_001103908.1
V1bR	Vasopressin 1b receptor	*Mus musculus*, *Gallus gallus*	NP_036054.1, NP_001026669.1
V2R	Vasopressin 2 receptor	*Mus musculus*, *Gallus gallus*	NP_062277.1, NP_001026650.1
VP/OT-like receptor	Vasopressin/Oxytocin-like receptor	*Daphnia pulex*	EFX69326.1

[a]Transcript ID number in the *Nematostella vectensis* genome database v1.0 (*genome.jgi-psf.org/Nemve1).*

Table S2.

Conservation of VP/OT-like peptide features in *C. elegans* nematocin.

Name	Peptide sequence [a]	Source	Ref.
arg-vasopressin [b]	CYFQNCPRG-----amide	mammals	(*52*)
lys-vasopressin	CYFQNCPKG-----amide	pig, some marsupials	(*53*)
phenypressin	CFFQNCPRG-----amide	some marsupials	(*54*)
vasotocin	CYIQNCPRG-----amide	nonmammalian vertebrates	(*55*)
oxytocin [b]	CYIQNCPLG-----amide	mammals	(*56*)
mesotocin	CYIQNCPIG-----amide	nonmammalian vertebrates [c]	(*57*)
isotocin	CYISNCPIG-----amide	bony fishes	(*58*)
echinotocin	CFISNCPKG-----amide	echinoderms	(*59*)
lys-conopressin	CFIRNCPKG-----amide	leech, various mollusks	(*60*)
cephalotocin	CYFRNCPIG-----amide	*Octopus vulgaris*	(*61*)
octopressin	CFWTSCPIG-----amide	*Octopus vulgaris*	(*62*)
inotocin	CLITNCPRG-----amide	insects	(*4*)
annetocin	CFVRNCPIG-----amide	annelids	(*63*)
nematocin	CFLNSCPYRRY---amide	nematodes	
Styela OT-related peptide	CYISDCPNSRFWSTamide	*Styela plicata*	(*64*)
Ciona VP/OT-related peptide	CFFRDCSNMDWYR------	*Ciona intestinalis*	(*65*)

[a]All VP/OT-related peptide sequences are cyclic with a disulfide bridge between Cys[1] and Cys[6]. Identical residues, black; conserved residues, dark grey; similar residues, light grey.

[b]VP-like peptides are characterized by a basic residue at position 8, while a neutral residue at this site is typical of OT-like peptides.

[c]lungfishes, amphibians, reptiles, birds, some marsupials

Table S3.

Accession numbers of VP/OT-related precursors.

Precursor	Species	Accession number
Vasopressin	*Homo sapiens*	AAA61291.1
Oxytocin	*Homo sapiens*	NP_000906.1
Conopressin	*Lymnea stagnalis*	AAB35220.1
Inotocin	*Tribolium castaneum*	NP_001078831.1
Nematocin	*Caenorhabditis elegans*	AFJ42491
	Caenorhabditis briggsae	XP_002644603.1
	Caenorhabditis remanei	XP_003118316.1
	Caenorhabditis brenneri	EGT30208.1
	Caenorhabditis japonica	H2WG31
	Pristionchus pacificus	H3EIQ3
	Necator americanus[a]	BU089245.1
	Ancylostoma caninum[a]	EY469192.1, EY465679.1
	Strongyloides stercoralis[a]	BE029002.1
	Bursaphelenchus xylophilus[a]	CJ991987.1, CJ988870.1

[a] Protein sequences were derived from EST sequence data.

Movie S1.
3D movie created from confocal Z-stack projections of a transgenic L1 hermaphrodite worm (wild type background) expressing the *ntc-1::gfp* transgene.

Movie S2.
3D movie created from confocal Z-stack projections of a transgenic L1 hermaphrodite worm (wild type background) expressing the *ntr-1::gfp* transgene.

Movie S3.
3D movie created from confocal Z-stack projections of a transgenic L1 hermaphrodite worm (wild type background) expressing the *ntr-2::gfp* transgene.

References (*22-65*)

22. S. Brenner, The genetics of *Caenorhabditis elegans*. *Genetics* **77**, 71-94 (1974).

23. T. Janssen *et al.*, Discovery of a cholecystokinin-gastrin-like signaling system in nematodes. *Endocrinology* **149**, 2826-2839 (2008).

24. B. Tursun, L. Cochella, I. Carrera, O. Hobert, A toolkit and robust pipeline for the generation of fosmid-based reporter genes in *C. elegans*. *PLoS One* **4**, e4625- (2009).

25. O. Hobert, PCR fusion-based approach to create reporter gene constructs for expression analysis in transgenic *C. elegans*. *Biotechniques* **32**, 728-730 (2002).

26. J. H. Chou, C. I. Bargmann, P. Sengupta, The *Caenorhabditis elegans odr-2* gene encodes a novel Ly-6-related protein required for olfaction. *Genetics* **157**, 211-224 (2001).

27. O. Hobert, T. D'Alberti, Y. Liu, G. Ruvkun, Control of neural development and function in a thermoregulatory network by the LIM homeobox gene *lin-11*. *J. Neurosci.* **18**, 2084-2096 (1998).

28. R. Baumeister, Y. Liu, G. Ruvkun, Lineage-specific regulators couple cell lineage asymmetry to the transcription of the *Caenorhabditis elegans* POU gene *unc-86* during neurogenesis. *Genes Dev.* **10**, 1395-1410 (1996).

29. R. R. Zwaal, J. E. Mendel, P. W. Sternberg, R. H. Plasterk, Two neuronal G proteins are involved in chemosensation of the *Caenorhabditis elegans* Dauer-inducing pheromone. *Genetics* **145**, 715-727 (1997).

30. S. Yu, L. Avery, E. Baude, D. L. Garbers, Guanylyl cyclase expression in specific sensory neurons: a new family of chemosensory receptors. *Proc. Natl. Acad. Sci. U. S. A* **94**, 3384-3387 (1997).

31. A. Sagasti, O. Hobert, E. R. Troemel, G. Ruvkun, C. I. Bargmann, Alternative olfactory neuron fates are specified by the LIM homeobox gene *lim-4*. *Genes Dev.* **13**, 1794-1806 (1999).

32. Z. Altun-Gultekin *et al.*, A regulatory cascade of three homeobox genes, *ceh-10*, *ttx-3* and *ceh-23*, controls cell fate specification of a defined interneuron class in *C. elegans*. *Development* **128**, 1951-1969 (2001).

33. E. R. Troemel, J. H. Chou, N. D. Dwyer, H. A. Colbert, C. I. Bargmann, Divergent seven transmembrane receptors are candidate chemosensory receptors in *C. elegans*. *Cell* **83**, 207-218 (1995).

34. S. J. Husson, E. Clynen, G. Baggerman, A. De Loof, L. Schoofs, Discovering neuropeptides in *Caenorhabditis elegans* by two dimensional liquid chromatography and mass spectrometry. *Biochem. Biophys. Res. Commun.* **335**, 76-86 (2005).

35. S. J. Husson *et al.*, in *Peptidomics: methods and protocols*, M. Soloviev, Ed. (Humana Press, New York, 2010), vol. 615, pp. 29-47.

36. I. Beets, M. Lindemans, T. Janssen, P. Verleyen, in *Neuropeptides: methods and protocols*, A. Merighi, Ed. (Humana Press, New York, 2011), vol. 789, pp. 377-391.

37. C. C. Mello, J. M. Kramer, D. Stinchcomb, V. Ambros, Efficient gene transfer in *C. elegans*: extrachromosomal maintenance and integration of transforming sequences. *EMBO J.* **10**, 3959-3970 (1991).

38. J. G. White, E. Southgate, J. N. Thomson, S. Brenner, The structure of the nervous system of the nematode *Caenorhabditis elegans*. *Philos. Trans. R Soc. London Ser. B* **314**, 1-340 (1986).

39. S. R. Wicks, C. J. de Vries, H. G. van Luenen, R. H. Plasterk, CHE-3, a cytosolic dynein heavy chain, is required for sensory cilia structure and function in *Caenorhabditis elegans*. *Dev. Biol.* **221**, 295-307 (2000).

40. F. Abascal, R. Zardoya, D. Posada, ProtTest: selection of best-fit models of protein evolution. *Bioinformatics* **21**, 2104-2105 (2005).

41. A. Drummond, K. Strimmer, PAL: an object-oriented programming library for molecular evolution and phylogenetics. *Bioinformatics* **17**, 662-663 (2001).

42. S. Guindon, O. Gascuel, A simple, fast, and accurate algorithm to estimate large phylogenies by maximum likelihood. *Syst. Biol.* **52**, 696-704 (2003).

43. R. Sanchez *et al.*, Phylemon 2.0: a suite of web-tools for molecular evolution, phylogenetics, phylogenomics and hypotheses testing. *Nucleic Acids Res.* **39**, W470-W474 (2011).

44. J. P. Huelsenbeck, F. Ronquist, MrBayes: Bayesian inference of phylogenetic trees. *Bioinformatics* **17**, 754-755 (2001).

45. F. Ronquist, J. P. Huelsenbeck, MrBayes 3: Bayesian phylogenetic inference under mixed models. *Bioinformatics* **19**, 1572-1574 (2003).

46. H. Akaike, A new look at the statistical model identification. *IEEE Trans. Autom. Contr.* **19**, 716-726 (1974).

47. S. Whelan, N. Goldman, A general empirical model of protein evolution derived from multiple protein families using a maximum-likelihood approach. *Mol. Biol. Evol.* **18**, 691-699 (2001).

48. The R Development Core Team, Eds., *R: a language and environment for statistical computing* (R foundation for statistical computing, Vienna, 2010).

49. M. Sharif, M. R. Hanley, Peptide receptors. Stepping up the pressure. *Nature* **357**, 279-280 (1992).

50. B. Mouillac *et al.*, The binding site of neuropeptide vasopressin V1a receptor. Evidence for a major localization within transmembrane regions. *J. Biol. Chem.* **270**, 25771-25777 (1995).

51. H. A. Colbert, T. L. Smith, C. I. Bargmann, OSM-9, a novel protein with structural similarity to channels, is required for olfaction, mechanosensation, and olfactory adaptation in *Caenorhabditis elegans*. *J. Neurosci.* **17**, 8259-8269 (1997).

52. R. Acher, J. Chauvet, La structure de la vasopressin de boeuf. *Biochim. Biophys. Acta* **12**, 487-488 (1953).

53. M. T. Chauvet, T. Colne, D. Hurpet, J. Chauvet, R. Acher, Marsupial neurohypophysial hormones: identification of mesotocin, lysine vasopressin, and phenypressin in the quokka wallaby (*Setonix brachyurus*). *Gen. Comp. Endocrinol.* **51**, 309-315 (1983).

54. M. T. Chauvet, D. Hurpet, J. Chauvet, R. Acher, Phenypressin (Phe2-Arg8-vasopressin), a new neurohypophysial peptide found in marsupials. *Nature* **287**, 640-642 (1980).

55. R. Acher, J. Chauvet, M. T. Lenci, F. Morel, J. Maetz, Présence d'une vasotocine dans la neurohypophyse de la grenouille (*Rana esculenta L.*). *Biochim. Biophys. Acta* **42**, 379-380 (1960).

56. V. du Vigneaud, C. Ressler, S. Trippett, The sequence of amino acids in oxytocin, with a proposal for the structure of oxytocin. *J. Biol. Chem.* **205**, 949-957 (1953).

57. R. Acher, J. Chauvet, Structure, processing and evolution of the neurohypophysial hormone-neurophysin precursors. *Biochimie* **70**, 1197-1207 (1988).

58. R. Acher, J. Chauvet, M. T. Chauvet, D. Crepy, Isolement d'une nouvelle hormone neurohypophysaire, l'isotocine, présente chez les poissons osseux. *Biochim. Biophys. Acta* **58**, 624-625 (1962).

59. M. R. Elphick, M. L. Rowe, NGFFFamide and echinotocin: structurally unrelated myoactive neuropeptides derived from neurophysin-containing precursors in sea urchins. *J. Exp. Biol.* **212**, 1067-1077 (2009).

60. M. Salzet, P. Bulet, A. Van Dorsselaer, J. Malecha, Isolation, structural characterization and biological function of a lysine-conopressin in the central nervous system of the pharyngobdellid leech *Erpobdella octoculata*. *Eur. J. Biochem.* **217**, 897-903 (1993).

61. G. Reich, A new peptide of the oxytocin/vasopressin family isolated from nerves of the cephalopod *Octopus vulgaris*. *Neurosci. Lett.* **134**, 191-194 (1992).

62. K. Takuwa-Kuroda, E. Iwakoshi-Ukena, A. Kanda, H. Minakata, Octopus, which owns the most advanced brain in invertebrates, has two members of vasopressin/oxytocin superfamily as in vertebrates. *Regul. Pept.* **115**, 139-149 (2003).

63. T. Oumi *et al.*, Annetocin, an annelid oxytocin-related peptide, induces egg-laying behavior in the earthworm, *Eisenia foetida*. *J. Exp. Zool.* **276**, 151-156 (1996).

64. K. Ukena, E. Iwakoshi-Ukena, A. Hikosaka, Unique form and osmoregulatory function of a neurohypophysial hormone in a urochordate. *Endocrinology* **149**, 5254-5261 (2008).

65. T. Kawada, T. Sekiguchi, Y. Itoh, M. Ogasawara, H. Satake, Characterization of a novel vasopressin/oxytocin superfamily peptide and its receptor from an ascidian, *Ciona intestinalis*. *Peptides* **29**, 1672-1678 (2008).